telecom

MDPI

Article

A 77 GHz Transmit Array for In-Package Automotive Radar Applications

Francesco Greco, Emilio Arnieri *, Giandomenico Amendola, Raffaele De Marco and Luigi Boccia

Millimeter-Wave Antennas and Integrated Circuits Laboratory (MAIC), University of Calabria DIMES, 87036 Quattromiglia, CS, Italy; f.greco@dimes.unical.it (F.G.); g.amendola@dimes.unical.it (G.A.); raffaele.demarco@dimes.unical.it (R.D.M.); luigi.boccia@unical.it (L.B.)
* Correspondence: emilio.arnieri@unical.it

Abstract: A packaged transmit array (TA) antenna is designed for automotive radar applications operating at 77 GHz. The compact dimensions of the proposed configuration make it compatible with standard quad flat no-lead package (QFN) technology. The TA placed inside the package cover is used to focus the field radiated by a feed placed in the same package. The unit cell of the array is composed of two pairs of stacked patches separated by a central ground plane. A planar patch antenna surrounded by a mushroom-type EBG (Electromagnetic Band Gap) structure is used as the primary feed. An analytical approach is employed to evaluate the primary parameters of the suggested TA, including its directivity, gain and spillover efficiency. The final design has been refined using comprehensive full-wave simulations. The simulated gain is 14.2 dBi at 77 GHz, with a half-power beamwidth of 22°. This proposed setup is a strong contender for highly integrated mid-gain applications in the automotive sector.

Keywords: transmit array; radar sensor; automotive

Citation: Greco, F.; Arnieri, E.; Amendola, G.; De Marco, R.; Boccia, L. A 77 GHz Transmit Array for In-Package Automotive Radar Applications. *Telecom* **2024**, *5*, 792–803. https://doi.org/10.3390/telecom5030040

Academic Editor: Minseok Kim

Received: 24 July 2024
Revised: 6 August 2024
Accepted: 12 August 2024
Published: 14 August 2024

1. Introduction

Currently, in the automotive industry, vehicles are controlled using different systems like pedestrian detection, adaptive cruise control, radars for lane keeping, blind spot detection and collision alerts. In particular, the increasing interest in autonomous driving vehicles requires reliable radar sensors. For this reason, it is predictable that the demand for automotive radars will keep rising in the near future. In recent years, the industry has focused its attention on 79 GHz radar systems, which extend the range of the previous 77 GHz radars (76–77 GHz) to include the 77–81 GHz range [1].

Automotive radar systems, like collision avoidance radars or intelligent cruise control (ICC), are based on antennas with high directivity. This characteristic is fundamental to increasing their capability of distinguishing targets in a specified field of view. Generally, for medium- and short-range radars, 3 dB beamwidths of ±40° to ±80° in azimuth and ±5° to ±12° in elevation are required in antennas [1]. Another important requirement of modern automotive radar systems is related to the antenna's ease of integration [2]. Radiators need to provide a low profile, be lightweight and have low manufacturing costs. In this context, printed antenna arrays appear to be a natural choice [1,3–5]; however, they may suffer from larger feed network losses. Free-space beam-forming techniques based on substrate lenses [6,7], transmit arrays [8] or reflect arrays [9] have been proposed in the literature to address this problem. It is well known that the performances of reflect arrays are limited by the blockage of the feed source, while substrate lenses are typically bulky and heavy. On the other hand, solutions based on transmit arrays can be considered a good solution for increasing the directivity of antenna systems while maintaining low weight and a low profile.

A transmit array is a phase-shifting surface consisting of unit cells. These can be used to focus the waves radiated by a feeding antenna into a narrower beamwidth. A progressive

phase shift is applied across the aperture of the transmit array, and in this manner the beam can be controlled and focused/steered towards a direction away from the boresight. Several examples of focusing transmit arrays are available in the literature. For example, in [10–12], focusing is obtained using arrays of transmit/receive antennas connected through transmission line sections of appropriate lengths.

This work uses a transmit array to focus the beam radiated by a package-integrated antenna. PCB space and low-cost assembly are critical for automotive applications; for this reason, package-integrated antennas can be an ideal choice for these space-constrained applications. In particular, the quad flat no-lead (QFN) packaging technique offers easier component placement as well as improved strength, reliability and thermal characteristics. The QFN packaging technique is a lead frame (LF)-based plastic package that has been widely used in the semiconductor industry since its introduction. This technique has several advantages, such as a cost-efficient packaging process with high heat dissipation properties and a simple production process [13–15].

The solution presented in this work is compact and perfectly compatible with QFN packaging technology for 77 GHz applications [4]. The proposed configuration demonstrates how a standard antenna with low directivity can be used as the feed for a transmit array (TA) with all components integrated into a standard QFN package. The antenna is incorporated into the package cover. This setup allows for the implementation of various integration methods, such as using an on-chip integrated feed or a feed array structure.

Compared to other solutions available in the recent literature, like the ones described in [6,7], the proposed solution is more compact and lightweight, while the solution proposed in [9] suffers from the blockage effect.

The design procedure is based on an analytical model of a transmit array to optimize several antenna parameters like gain, but also the focal distance over aperture size (f/D). The final structure has been integrated into a 12 $\times$ 12 mm^2 QFN [13,15,16] open-cavity package. The proposed design approach allows us to place the transmit array elements very close to the feed ($f/D = 0.5$), allowing for a highly integrated structure compatible with QFN technology.

The high gain and integration properties of the proposed transmit array are promising for automotive radar applications. The preliminary results were presented by the authors in [17].

2. Transmit Array Design

The overall structure of the proposed transmit array is presented in Figure 1. A planar patch antenna surrounded by a mushroom-type EBG (Electromagnetic Band Gap) structure is used as the primary feed. The proposed configuration was designed to be integrated into a $W \times W$ (12 $\times$ 12 mm^2) package using QFN technology. The feed is in the centre of the package, while the package cover is positioned at a distance of f = 2 mm. The following sections will provide a detailed description of the feed antenna and transmit array.

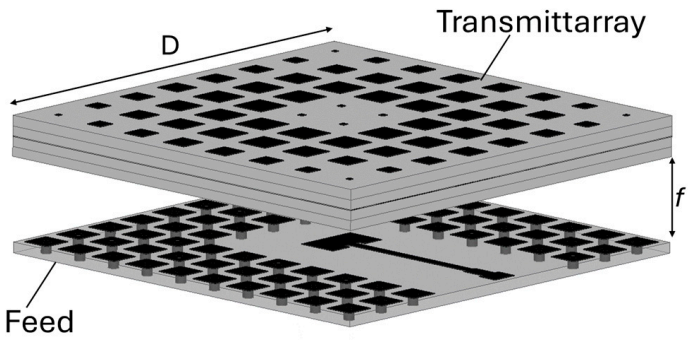

Figure 1. Transmit array's antenna configuration.

2.1. Antenna Feed

A planar antenna configuration is used as the primary feed to realize a low-cost, integrated, 77 GHz RF, front-end package for automotive applications, integrable into a transceiver module. The transmit array fed can be either monolithically integrated onto the chip [18] or printed on a standard substrate. In this paper, a standard printed antenna is employed (Figure 2). A conventional patch antenna with an inset feed has been designed to resonate at the central frequency of the band. The patch is printed on a 0.25 mm Rogers RO3003 substrate with DK = 3 and a dissipation factor of 0.0010.

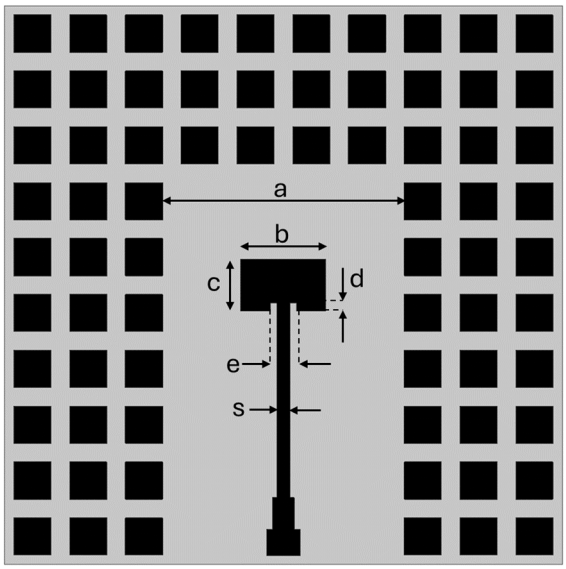

Figure 2. Feeding patch antenna with EBG structure. a = 4.55 mm; b = 1.6 mm; c = 0.98 mm; d = 0.15 mm; e = 0.5 mm; s = 0.25 mm.

One of the main problems associated with this type of configuration is the excitation of surface waves, which cause a deterioration of the radiation pattern. It is well known that the suppression of the surface waves improves the antenna performance, increasing the energy radiated in the broadside direction. To suppress the propagation of surface waves, the radiating patch has been surrounded by a mushroom-type EBG (Electromagnetic Band Gap) structure [19–21].

The EBG has been designed to provide a band gap able to cover the whole antenna bandwidth. In this manner, the surface waves launched from the antenna inside the substrate are efficiently suppressed. The mushroom-type EBG [22] is composed of metallic patches with central vias, as shown in Figure 3. This type of structure exhibits unique electromagnetic properties with a bandgap characteristic that is mainly determined by the patch and gap width, substrate permittivity, substrate thickness and metal vias' radius.

To evaluate the band gap proprieties of the EBG, a dispersion diagram of the mushroom-type structure's unit cell has been generated. The parameters have been tuned to create a band gap able to cover the band of interest. An LC filter array can be used for the explanation of the operation mechanism of the EBG structure. An increment in patch width *Wp* and decrement in gap (*Dp*-*Wp*), while keeping the height and permittivity of the substrate fixed, causes an increment in capacitance, which results in the decrement of the structure's resonant frequency. Figure 3 shows the dispersion diagram obtained with *Dp* = 1.05 mm; *Wp* = 0.7 mm; and via a diameter of 0.254 mm. A large stop band is created on the periodic surface from 60 GHz to 82 GHz.

In order to improve the transmit array's performance, a flat radiation pattern over a large angular range is preferable. To this end, the patch antenna has been surrounded by three rows of mushroom-type EBGs, as shown in Figure 2. The normalized radiation patterns of the patch antenna with and without EBGs are compared in Figure 4. A noticeable

improvement in terms of the radiation pattern's flatness is observed: the −3 dB beamwidth has been increased from 14° to about 90°. The smoother pattern is more suited to being a feed for the transmit array. The feeding patch has a gain of 7.5 dBi.

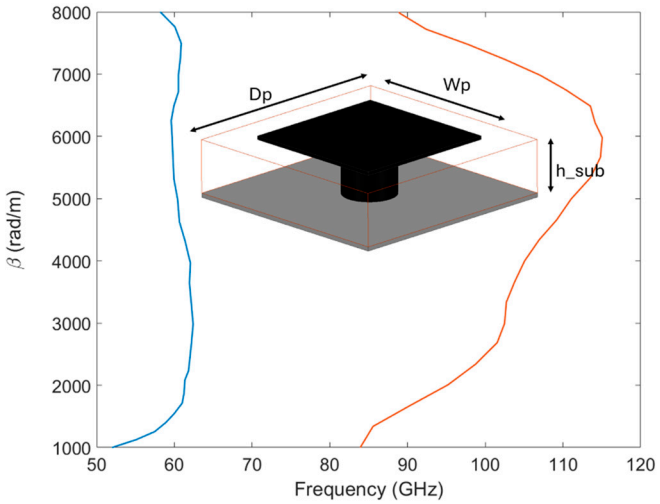

Figure 3. Dispersion diagram of the unit cell EBG structure printed on a Rogers RO3003 substrate. Dp = 1.05 mm; Wp = 0.7 mm; h_sub = 0.25 mm. Blue line: first mode; orange line: second mode.

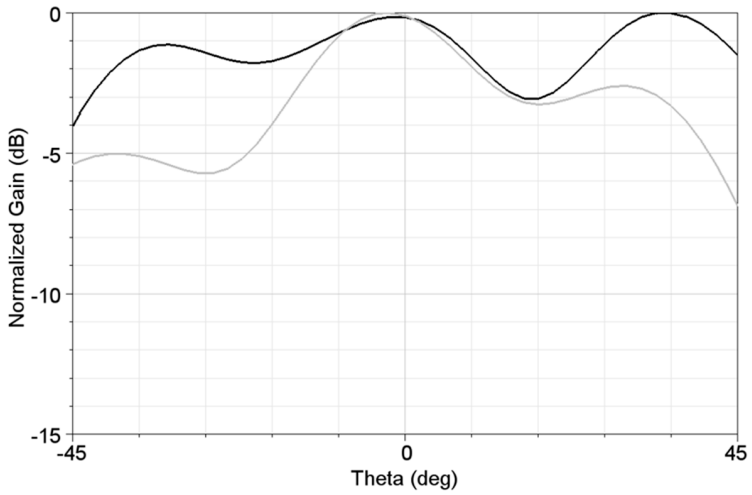

Figure 4. Normalized radiation patterns (E-plane) of the patch antenna with (black line) and without (grey line) mushroom-type EBGs.

2.2. Transmit Array Unit Cell

A slot-fed stacked patch antenna [23] was used as a transmit array unit cell, as shown in Figure 5. From previous research [24], it is well known that a slot-fed stacked patch antenna can be used to enhance the directivity of a radiated field if properly dimensioned. Two pairs of stacked patches are separated by a central ground plane. The lower square patches are used as receiving elements while the upper radiators are used as transmitting elements. In the proposed configuration, the receiving patches face the focal source, while the transmitting patches face the free space. An aperture (slot) is used in the central ground plane to couple the receiving elements on their lower side, with the transmitting ones placed on the opposite side of the transmit array. The patches are printed on a 0.2 mm Arlon AD350A with a dielectric constant $\varepsilon_r = 3.55$ and a loss tangent of 0.0033. The four patches have the same dimensions. The phase response is controlled by changing the side lengths of all the stacked patches. Unit cells with different patch lengths can be arranged to provide a desired phase distribution across the array surface. The unit cell's periodicity is W = 1.35 mm (0.35 λ_0 at 77 GHz) for both planes.

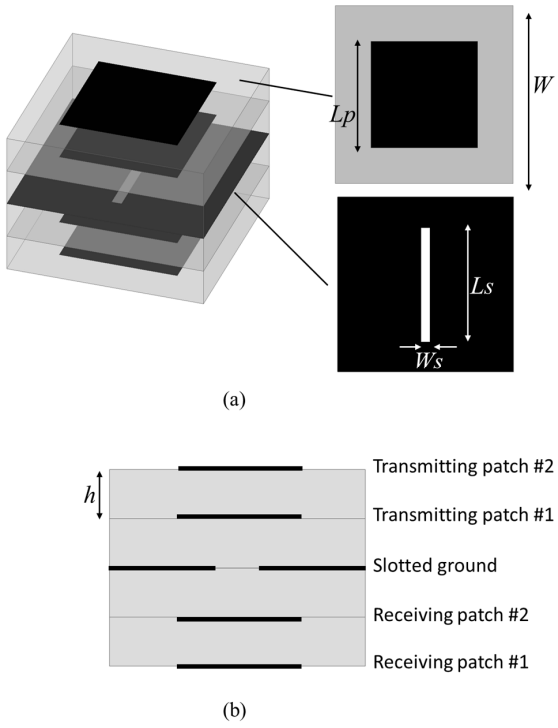

Figure 5. Transmit array unit cell structure. (**a**) 3D vies; (**b**) side view.

In Figure 6, the fields radiated from the unit cell with different angles of incidence are plotted in terms of magnitude and phase. The structure has highly stable behaviour for incidence angles up to 60°. This characteristic can be used to reduce the f/D of the proposed configuration.

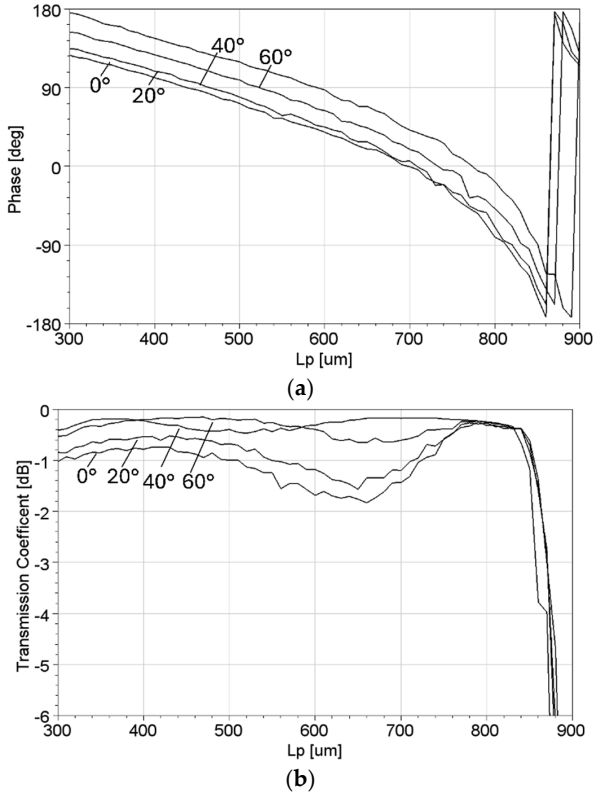

Figure 6. Simulated S21 in terms of phase (**a**) and magnitude (**b**) as a function of patch size (Lp) for different angles of incidence.

3. Analytical Model

A transmit array analytical model based on the evaluation of power transfers [10] is used in this paper. Four parameters have been considered to compute the TA's efficiency (Figure 7): P_1 is the power at the input of the focal source, while P_2 is the power radiated by the same source. P_3 is the incident power collected by the receiving side of the transmit array. Finally, P_4 is the power re-radiated from the transmission side of the array. The antenna efficiency is defined as follows:

$$\eta = \frac{P_4}{P_1} = \eta_{FS}\eta_{SO}\eta_{IL}$$

where η_{FS} is the realized efficiency of the focal array (P_2/P_1), η_{SO} is the spillover efficiency (P_3/P_2) and η_{IL} is the insertion loss of the unit cell (P_4/P_3). To enhance directivity and spillover efficiency, it is essential to examine the behaviour of the transmit array versus variations in its design parameters such as focal distance (f) and D, as well as the number and spacing of its elements. For simplicity, the feed's radiation pattern is assumed to be equal to $\cos^q \Theta$ with $q = 0.5$. Figure 8 illustrates the TA's performance in terms of spillover efficiency and gain for different f/D ratios, based on the previously discussed analytical model. The optimal performance is achieved when f/D equals 0.5. Additionally, the cell size is a crucial factor for a given f/D value. Figure 9 depicts how element spacing affects the transmit array's directivity. As shown, the directivity increases as the spacing between the elements decreases, leading to a chosen spacing of $\lambda/3$ to maximize directivity.

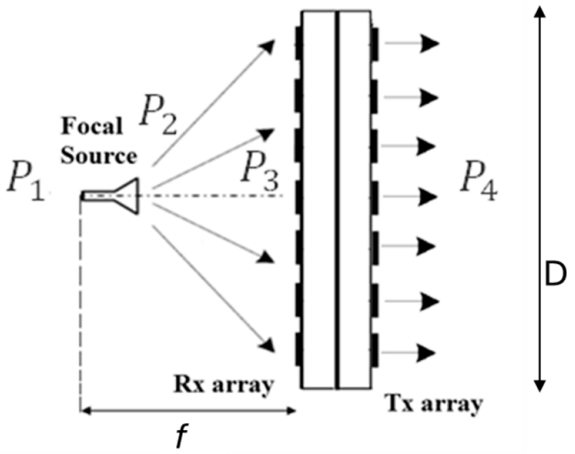

Figure 7. Transmit array geometry.

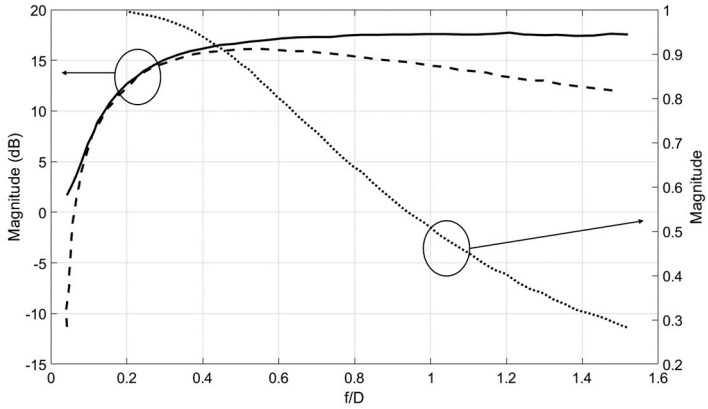

Figure 8. x8 array: calculated gain (dashed line), directivity (continuous line) and spillover efficiency (dotted line) for different values of f/D (spacing $\lambda/3$).

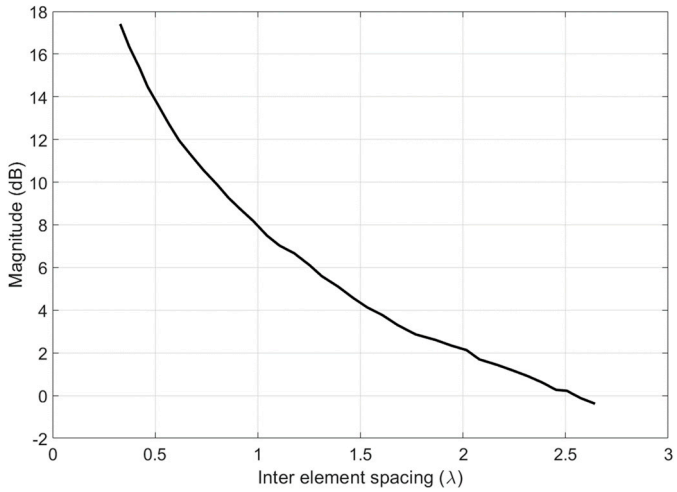

Figure 9. x8 array: calculated directivity of the unit cell as a function of inter-element spacing.

4. Results

The proposed analytical model was utilized to examine the relationships between the dimensions of the array, the focal length and the number of elements, as well as the behaviour of the transmit array in response to these variations. After defining all the parameters, the proposed configuration was simulated using Ansys HFSS [25]. The effect of the package has been included in the final model. The system comprises an 8×8 element transmit array with a spacing of $\lambda/3$ between elements. Each TA element has been dimensioned based on the results shown in Figure 6a to compensate for the phase differences of the signals coming from the feeding patch. Figure 10 presents the simulated radiation pattern of the antenna feed both with and without the transmit array.

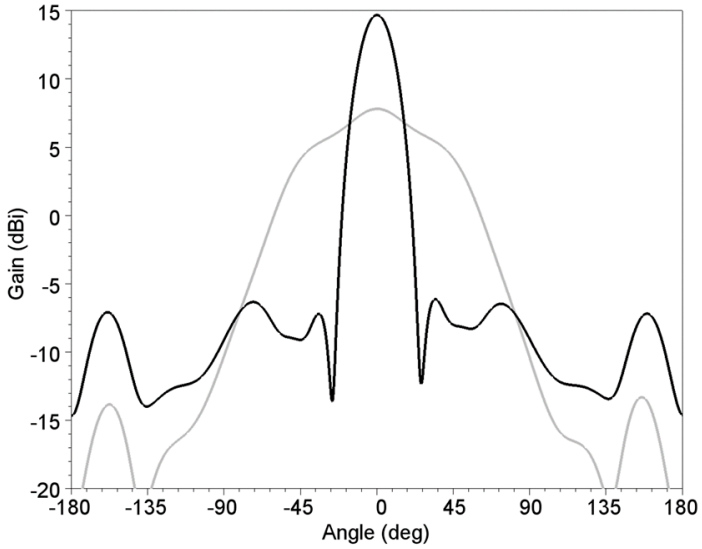

Figure 10. Simulated gain patterns (H plane) at 77 Hz for the EBG patch antenna with (black line) and without (gray line) a transmit array.

A prototype of the proposed transmit array configuration has been fabricated (Figure 11). To measure the antenna with WR10 waveguide equipment, a printed circuit board (PCB) launch connector (BN 533411, Spinner GmbH, Munich, Germany) has been used.

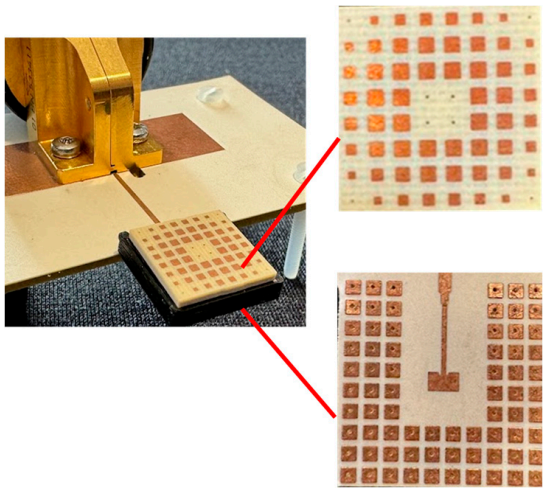

(**a**)

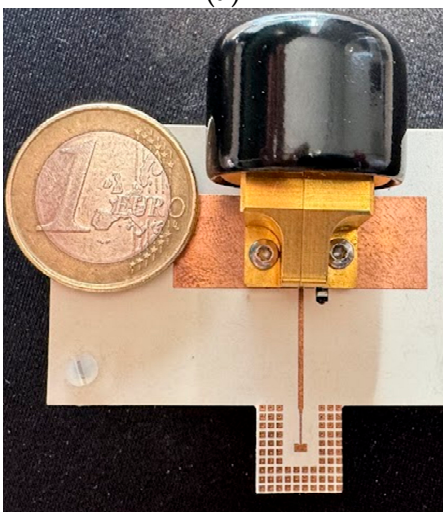

(**b**)

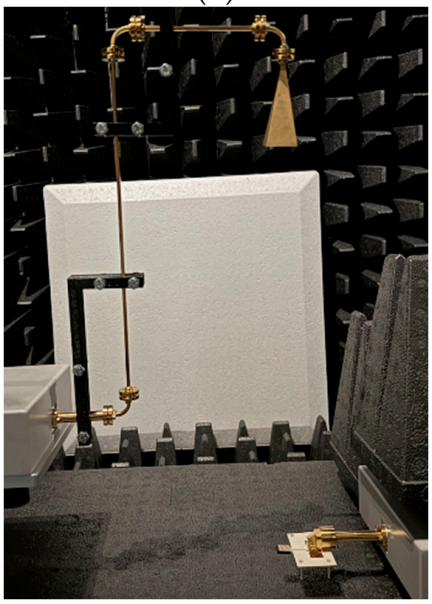

(**c**)

Figure 11. Fabricated prototype of the transmit array. (**a**) A 12 × 12 mm^2 package. (**b**) The feed patch with the EBG (**c**) measurement setup.

Figure 12 shows the simulated and measured matching of the fabricated prototype, while the radiation H-plane patterns are compared in Figure 13. the Simulated side lobes are lower than −20 dB. This is a value perfectly in line with those typically obtained from a high-performance transmit array. The E-plane patterns were not measured because of the limitations of the measurement setup. Minor discrepancies are visible in the measured beam, as well as a slightly higher side-lobe level. This can be attributed to several reasons like the PCB fabrication tolerances of the feeding patch or the Tas and the alignment of the lower patch to the upper TA and the transmit array to the feeding horn used in the high-frequency measurement setup (Figure 11c). However, the measured results agree quite well with the simulations. The measured gain is 14.2 dB at 77 GHz, with a 68% radiation efficiency and a First Null Beamwidth of 52.5°.

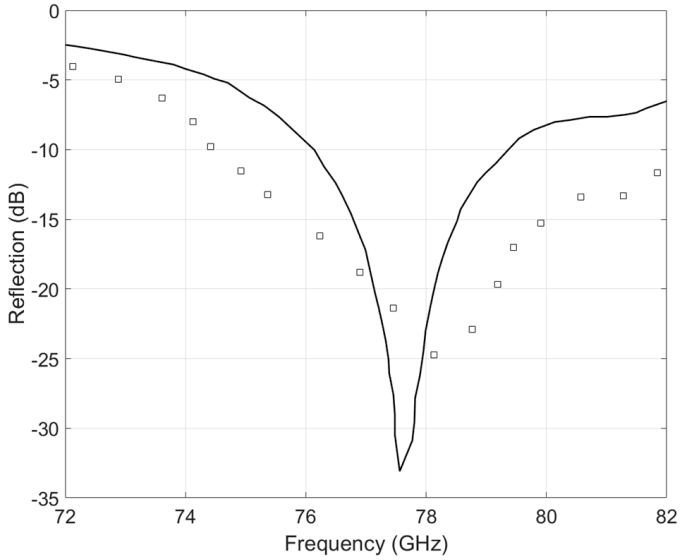

Figure 12. Simulated (continuous line) and measured (dots) reflection coefficients.

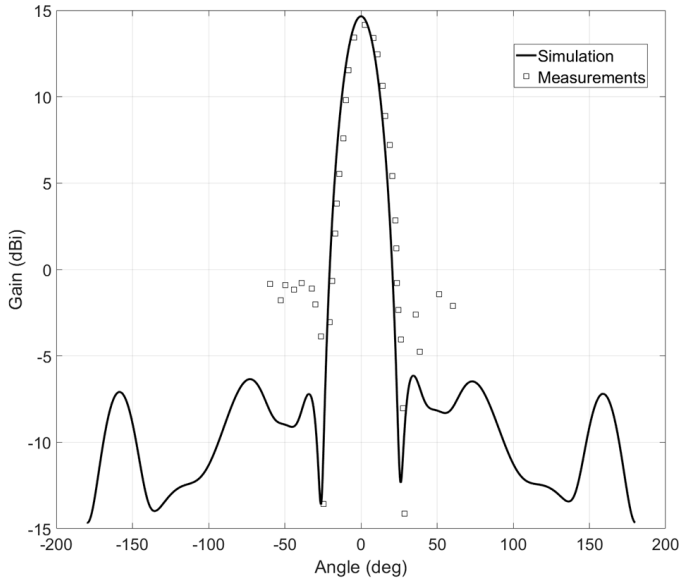

Figure 13. Transmit array radiation pattern: comparison between full-wave simulations and measurements. The measured gain is 14.2 dBi.

5. Discussion

In the literature, several array-based solution examples for automotive radar applications like those in [1,3–5] are available; however, they may suffer from larger feed network losses. If compared to other solutions based on a lens like the ones described in [6,7], our proposed configuration is more compact and lightweight, while the reflect array proposed in [9] suffers from the blockage effect. Solutions based on transmit arrays can be considered good solutions for increasing the directivity of the antenna systems while maintaining a low weight and low profile. In Table 1, the configuration proposed in this work is compared with other transmit arrays taken from the recent literature. The aperture efficiency of the proposed transmit array compares well with other solutions, while its compact side dimension (W = 12 mm) makes it compatible with QFN package integration.

Table 1. Transmit array comparison.

Ref.	Freq (GHz)	W (mm)	Eff (%)	Feed Type	QFN Compatible
[8]	76.5	40.35	5	Planar (SIW Slot)	NO
[26]	60	50	14.2	Not planar (Horn)	NO
[27]	77	46.55	19.7	Not planar (Horn)	NO
This Work	77	12	22	Planar (Patch)	YES

6. Conclusions

A 77 GHz packaged transmit array antenna for automotive radar applications has been presented. The whole structure is compact and realized in planar technology, which make it compatible with standard quad flat no-lead package (QFN) technology. A planar feed and a transmit array are both integrated into a single package. The electromagnetic field radiated by a feed is focused by the transmit array antenna placed on the package cover. The unit cell of the array is composed of two pairs of stacked patches separated by a central ground plane. The primary feed is realized with a planar patch antenna surrounded by a mushroom-type EBG. The relevant parameters of the proposed TA, like directivity, gain and spillover efficiency, have been evaluated using an analytical model. The final configuration has then been optimized by means of full-wave simulations. The simulated gain is 14.2 dBi at 77 Ghz, while the half-power beamwidth is 22°. The gain and beamwidth are in line with medium- and short-range automotive radar requirements [1,28]. The proposed transmit array is a good candidate for highly integrated mid-gain automotive applications.

Author Contributions: Conceptualization, L.B. and E.A.; software, F.G. and R.D.M.; validation, E.A.; formal analysis, F.G.; writing—original draft preparation, E.A.; writing, E.A. and F.G.; visualization, F.G.; supervision, G.A.; project administration, G.A.; funding acquisition, G.A. All authors have read and agreed to the published version of the manuscript.

Funding: This research received no external funding.

Data Availability Statement: Data is contained within the article.

Conflicts of Interest: The authors declare no conflict of interest.

References

1. Hasch, J.; Topak, E.; Schnabel, R.; Zwick, T.; Weigel, R.; Waldschmidt, C. Millimeter-Wave Technology for Automotive Radar Sensors in the 77 GHz Frequency Band. *IEEE Trans. Microw. Theory Tech.* **2012**, *60*, 845–860. [CrossRef]
2. Arnieri, E.; Boccia, L.; Amendola, G.; Glisic, S.; Mao, C.; Gao, S.; Rommel, T.; Penkala, P.; Krstic, M.; Yodprasit, U.; et al. An Integrated Radar Tile for Digital Beamforming X-/Ka-Band Synthetic Aperture Radar Instruments. *IEEE Trans. Microw. Theory Tech.* **2019**, *67*, 1197–1206. [CrossRef]
3. Menzel, W.; Moebius, A. Antenna Concepts for Millimeter-Wave Automotive Radar Sensors. *Proc. IEEE* **2012**, *100*, 2372–2379. [CrossRef]
4. Arnieri, E.; Greco, F.; Boccia, L.; Amendola, G. A Reduced Size Planar Grid Array Antenna for Automotive Radar Sensors. *IEEE Antennas Wirel. Propag. Lett.* **2018**, *17*, 2389–2393. [CrossRef]
5. Xu, J.; Hong, W.; Zhang, H.; Wang, G.; Yu, Y.; Jiang, Z.H. An Array Antenna for Both Long- and Medium-Range 77 GHz Automotive Radar Applications. *IEEE Trans. Antennas Propag.* **2017**, *65*, 7207–7216. [CrossRef]
6. Porter, B.; Rauth, L.; Mura, J.; Gearhart, S. Dual-polarized slot-coupled patch antennas on Duroid with teflon lenses for 76.5-GHz automotive radar systems. *IEEE Trans. Antennas Propag.* **1999**, *47*, 1836–1842. [CrossRef]
7. Saleem, M.K.; Vettikaladi, H.; Alkanhal, M.A.S.; Himdi, M. Lens Antenna for Wide Angle Beam Scanning at 79 GHz for Automotive Short Range Radar Applications. *IEEE Trans. Antennas Propag.* **2017**, *65*, 2041–2046. [CrossRef]
8. Yeap, S.B.; Qing, X.; Chen, Z.N. 77-GHz Dual-Layer Transmit-Array for Automotive Radar Applications. *IEEE Trans. Antennas Propag.* **2015**, *63*, 2833–2837. [CrossRef]
9. Park, Y.J.; Herschlein, A.; Wiesbeck, W. Offset cylindrical reflector antenna fed by a parallel-plate Luneburg lens for auto-motive radar applications in mm-wave. *IEEE Antennas Propag. Soc. Int. Symp.* **2002**, *4*, 588–591.
10. Pozar, D. Flat lens antenna concept using aperture coupled microstrip patches. *Electron. Lett.* **1996**, *32*, 2109–2111. [CrossRef]
11. McGrath, D. Planar three-dimensional constrained lenses. *IEEE Trans. Antennas Propag.* **1986**, *34*, 46–50. [CrossRef]
12. Popovic, D.; Popovic, Z. Multibeam antennas with polarization and angle diversity. *IEEE Trans. Antennas Propag.* **2002**, *50*, 651–657. [CrossRef]
13. Xi, J.; Xiao, F.; Wang, H. Comparative study on the reliability of QFN and AAQFN packages. In Proceedings of the 2014 15th International Conference on Electronic Packaging Technology, Chengdu, China, 12–15 August 2014; pp. 959–9620. [CrossRef]
14. Li, L. Reliability modeling and testing of advanced QFN packages'. In Proceedings of the 2013 IEEE 63rd Electronic Components and Technology Conference, Las Vegas, NV, USA, 28–31 May 2013; pp. 725–730. [CrossRef]
15. Lu, A.; Xie, D.; Shi, Z.; Ryu, W. Electrical and thermal modelling of QFN packages. In Proceedings of the 3rd Electronics Packaging Technology Conference (EPTC 2000) (Cat. No.00EX456), Singapore, 7 December 2000; pp. 352–356. [CrossRef]
16. U.S. Chip Packaging with Mil-Spec Precision. Available online: https://semiengineering.com/u-s-chip-packaging-with-mil-spec-precision/ (accessed on 29 September 2022).
17. Greco, F.; Boccia, L.; Amendola, G.; Arnieri, E. Design of an in-package transmit-array for automotive applications:preliminary results. In Proceedings of the 2022 Microwave Mediterranean Symposium (MMS), Pizzo Calabro, Italy, 9–13 May 2022; pp. 1–4. [CrossRef]
18. Mustacchio, C.; Boccia, L.; Arnieri, E.; Amendola, G. A Gain Levelling Technique for On-Chip Antennas Based on Split-Ring Resonators. *IEEE Access* **2021**, *9*, 90750–90756. [CrossRef]
19. Zaman, M.I.; Hamedani, F.T.; Amjadi, H. A New EBG structure and its application on microstrip patch antenna. In Proceedings of the 2012 15 International Symposium on Antenna Technology and Applied Electromagnetics, Toulouse, France, 25–28 June 2012; pp. 1–3. [CrossRef]
20. Sravya, R.V.; Kumari, R. Gain enhancement of patch antenna using L-slotted mushroom EBG. In Proceedings of the 2018 Conference on Signal Processing And Communication Engineering Systems (SPACES), Vijayawada, India, 4–5 January 2018; pp. 37–40. [CrossRef]
21. Neo, C.; Lee, Y.H. Patch antenna enhancement using a mushroom-like EBG structures. In Proceedings of the 2013 IEEE Antennas and Propagation Society International Symposium (APSURSI), Orlando, FL, USA, 7–13 July 2013; pp. 614–615. [CrossRef]
22. Sievenpiper, D. High-Impedance Electromagnetic Surfaces. Ph.D. Thesis, University of California, Los Angeles, CA, USA, 1999.
23. Plaza, E.; Leon, G.; Loredo, S.; Las-Heras, F. A Simple Model for Analyzing Transmitarray Lenses. *IEEE Antennas Propag. Mag.* **2015**, *57*, 131–144. [CrossRef]
24. Arnieri, E.; Amendola, G.; Boccia, L. Stacked shorted circular patch antenna in SIW technology for 60-GHz band arrays. In Proceedings of the 2017 IEEE International Symposium on Antennas and Propagation USNC/URSI National Radio Science Meeting, San Diego, CA, USA, 9–14 July 2017; pp. 2675–2676. [CrossRef]
25. Clemente, A.; Dussopt, L.; Sauleau, R.; Potier, P.; Pouliguen, P. Multiple feed transmit-array antennas with reduced focal distance. In Proceedings of the 2012 9th European Radar Conference, Amsterdam, The Netherlands, 30 October–1 November 2012; pp. 500–503.
26. Kaouach, H.; Dussopt, L.; Lanteri, J.; Koleck, T.; Sauleau, R. Wideband Low-Loss Linear and Circular Polarization Transmit-Arrays in V-Band. *IEEE Trans. Antennas Propag.* **2011**, *59*, 2513–2523. [CrossRef]

27. Vorobyov, A.; Fourn, E.; Sauleau, R.; Baghchehsaraei, Z.; Oberhammer, J.; Chicherin, D.; Raisanen, A. Iris-based 2-bit waveguide phase shifters and transmit-array for automotive radar applications. In Proceedings of the 2012 6th European Conference on Antennas and Propagation (EUCAP), Prague, Czech Republic, 26–30 March 2012; pp. 3711–3715. [CrossRef]
28. Bu, D.; Qu, S. Magneto-electric dipole antenna array for 77 GHz automotive radar. *IET Microw. Antennas Propag.* **2024**, *18*, 96–105. [CrossRef]